



Supplementary materials

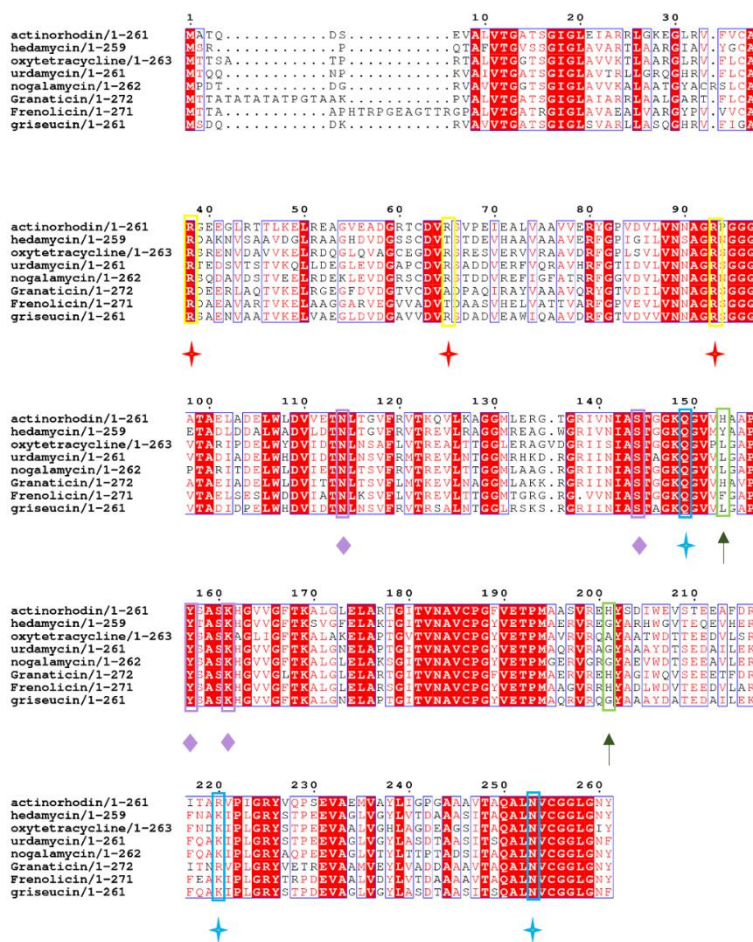
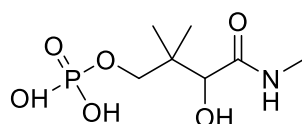
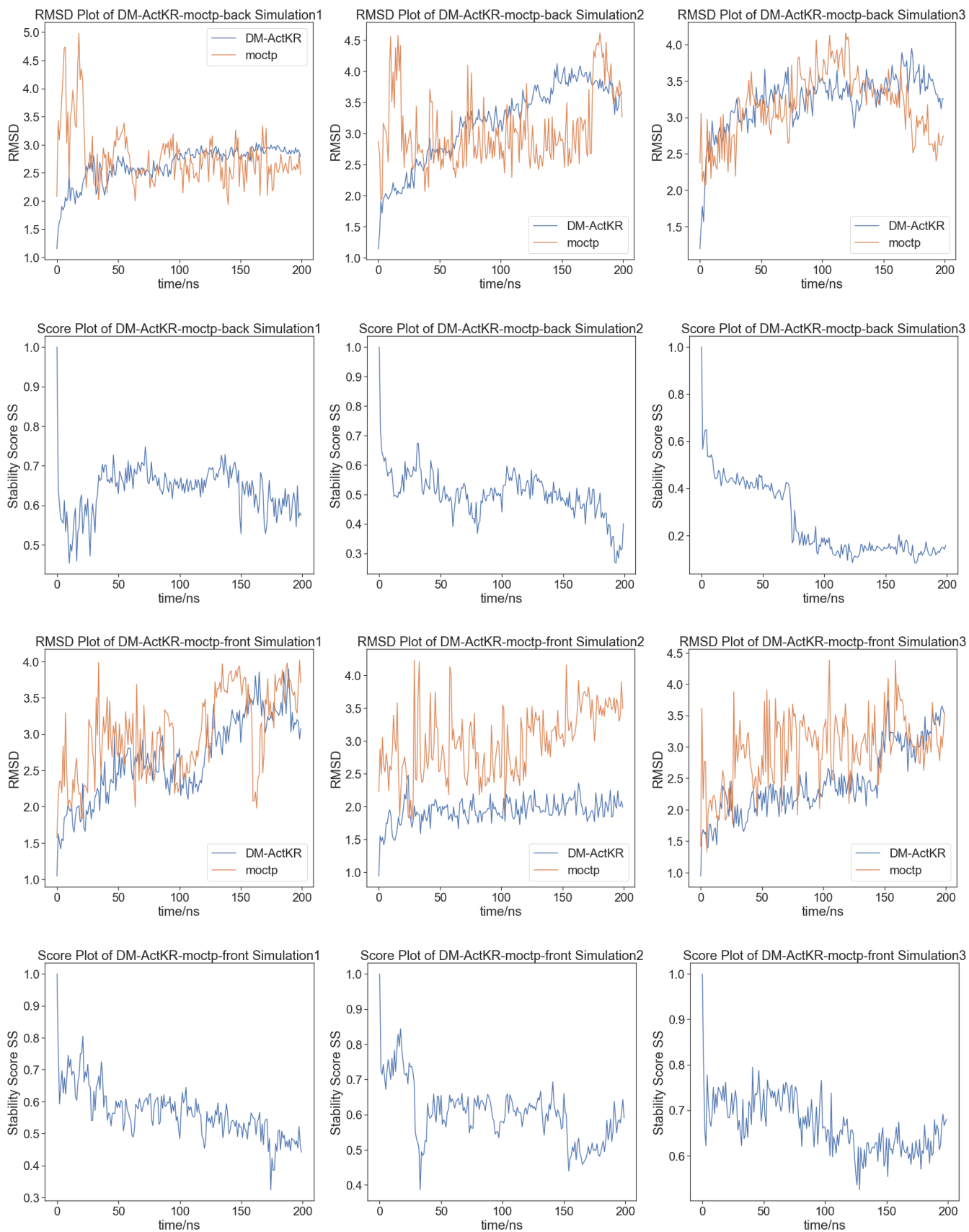


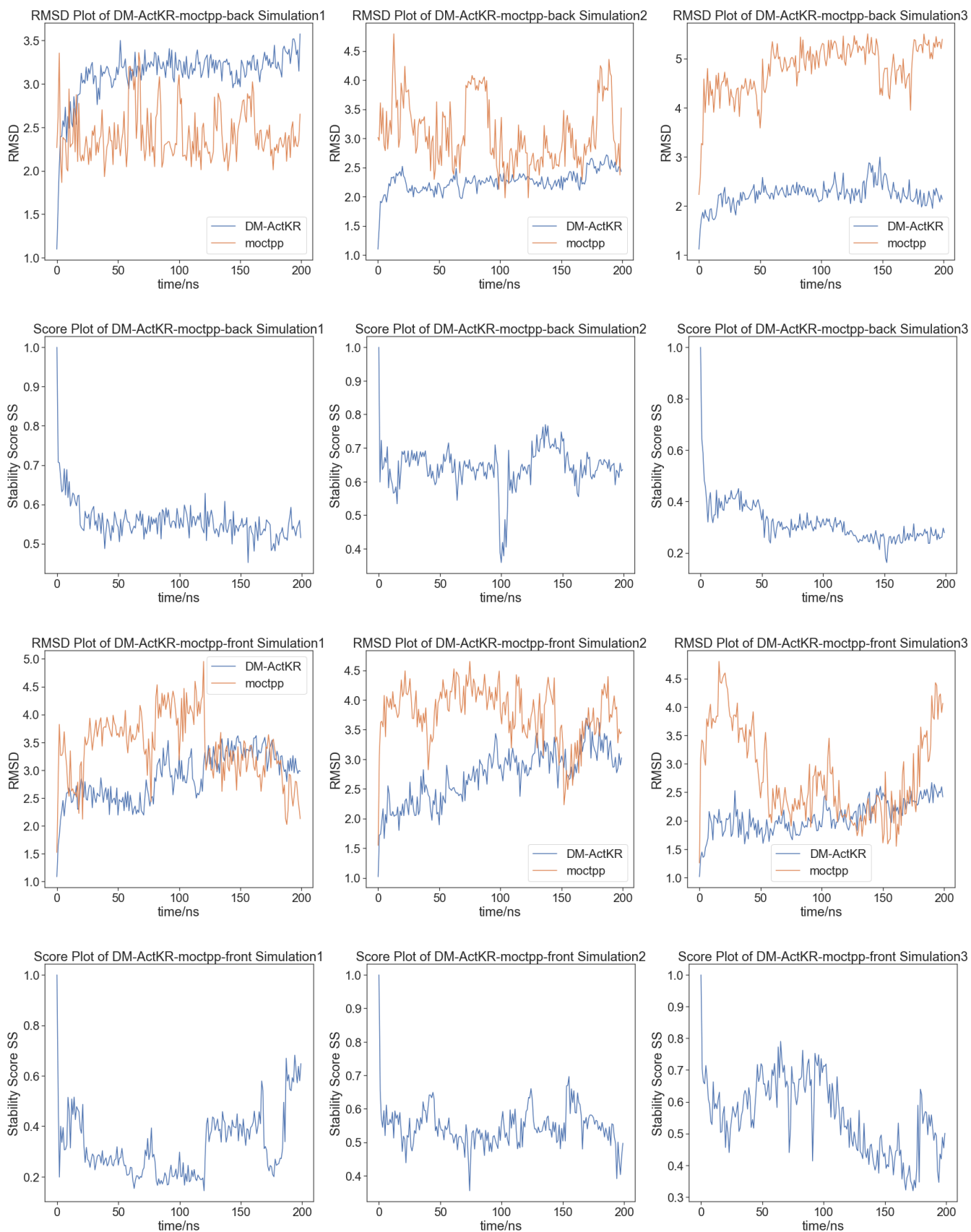
Figure S1. Sequence alignment among various type II PKS KR. Sequences included actinorhodin, hedamycin, oxytetracycline, urdamycin, nogalamycin, granaticin, frenolicin, and griseucic KR. Key: Red stars, front-patch residues; Cyan stars, back-patch residues; Purple diamonds, catalytic residues; Green arrows, proposed chain length filter residues (double mutation targets on WT-*ActKR*).

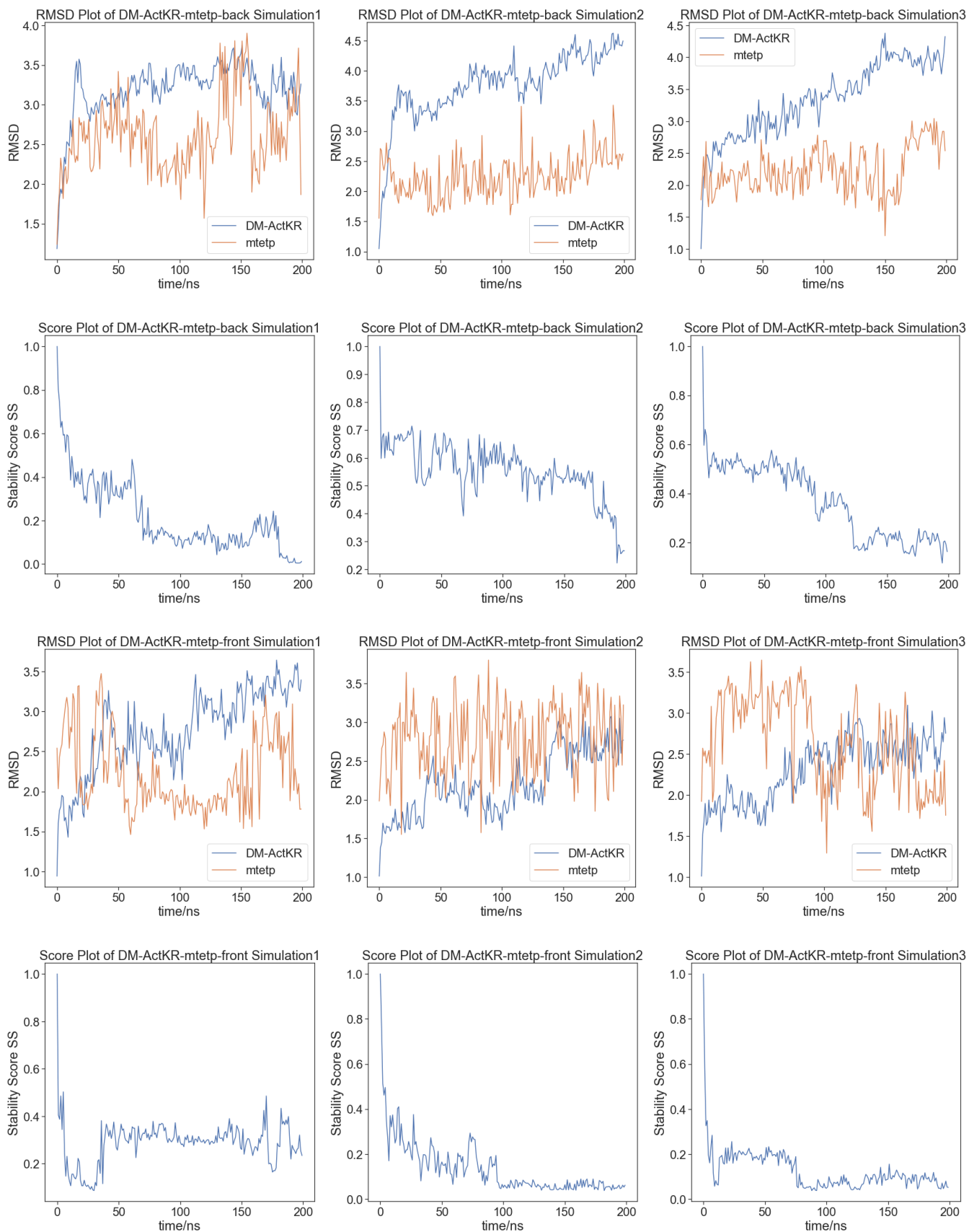


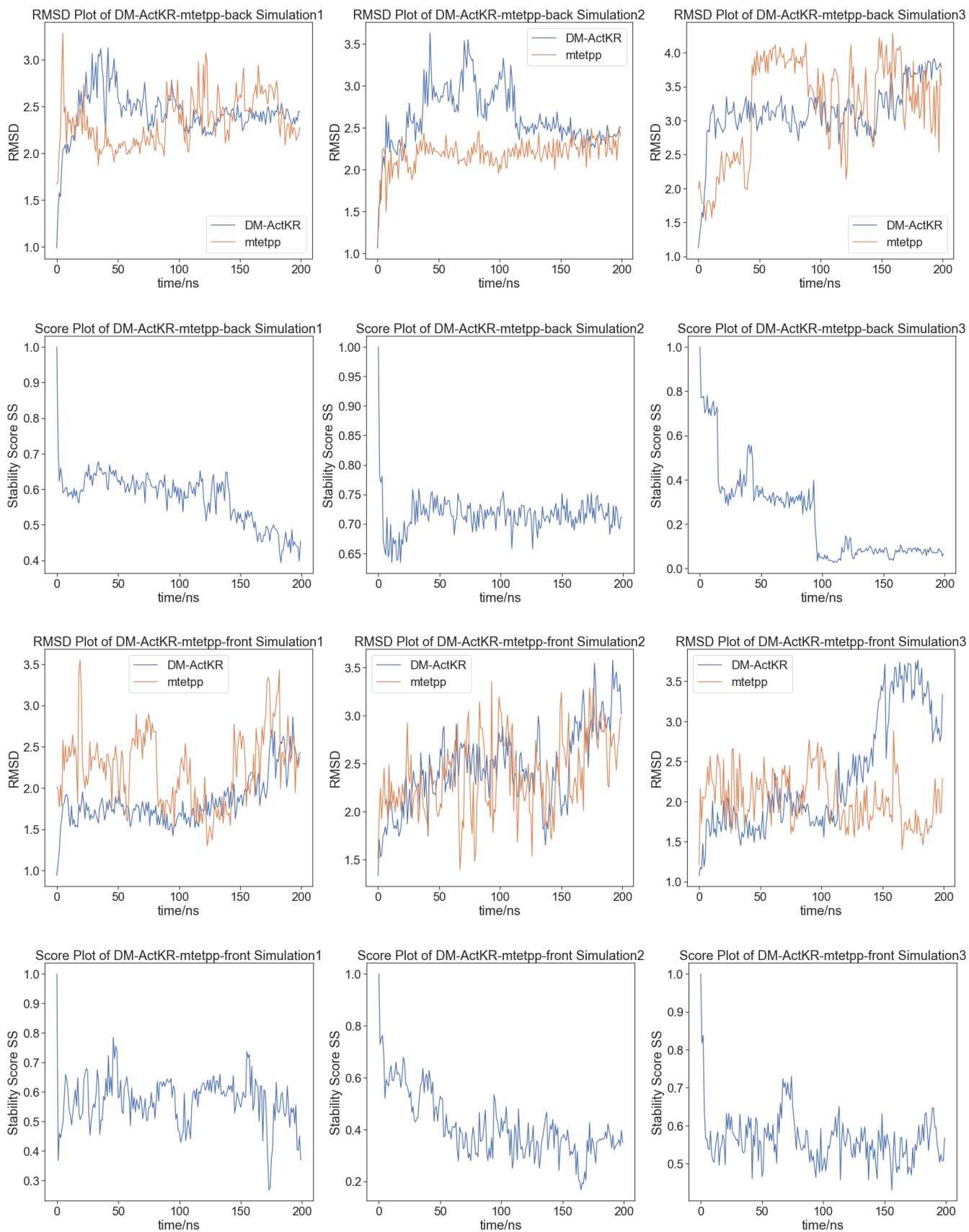
3-hydroxy-2,2-dimethyl-4-(methylamino)-4-oxobutyl dihydrogen phosphate

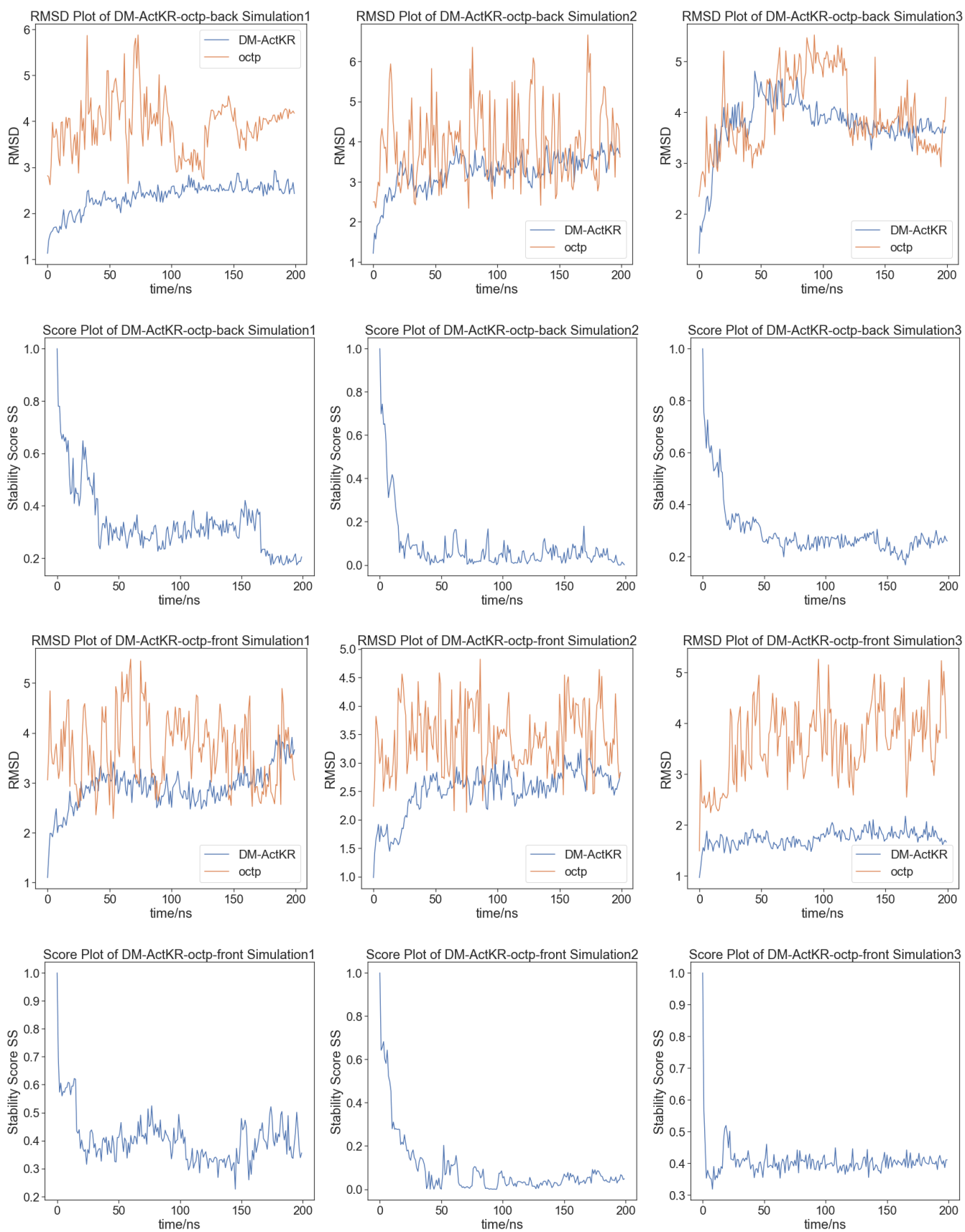
Figure S2. The phosphopantetheine fragment used in molecular docking.

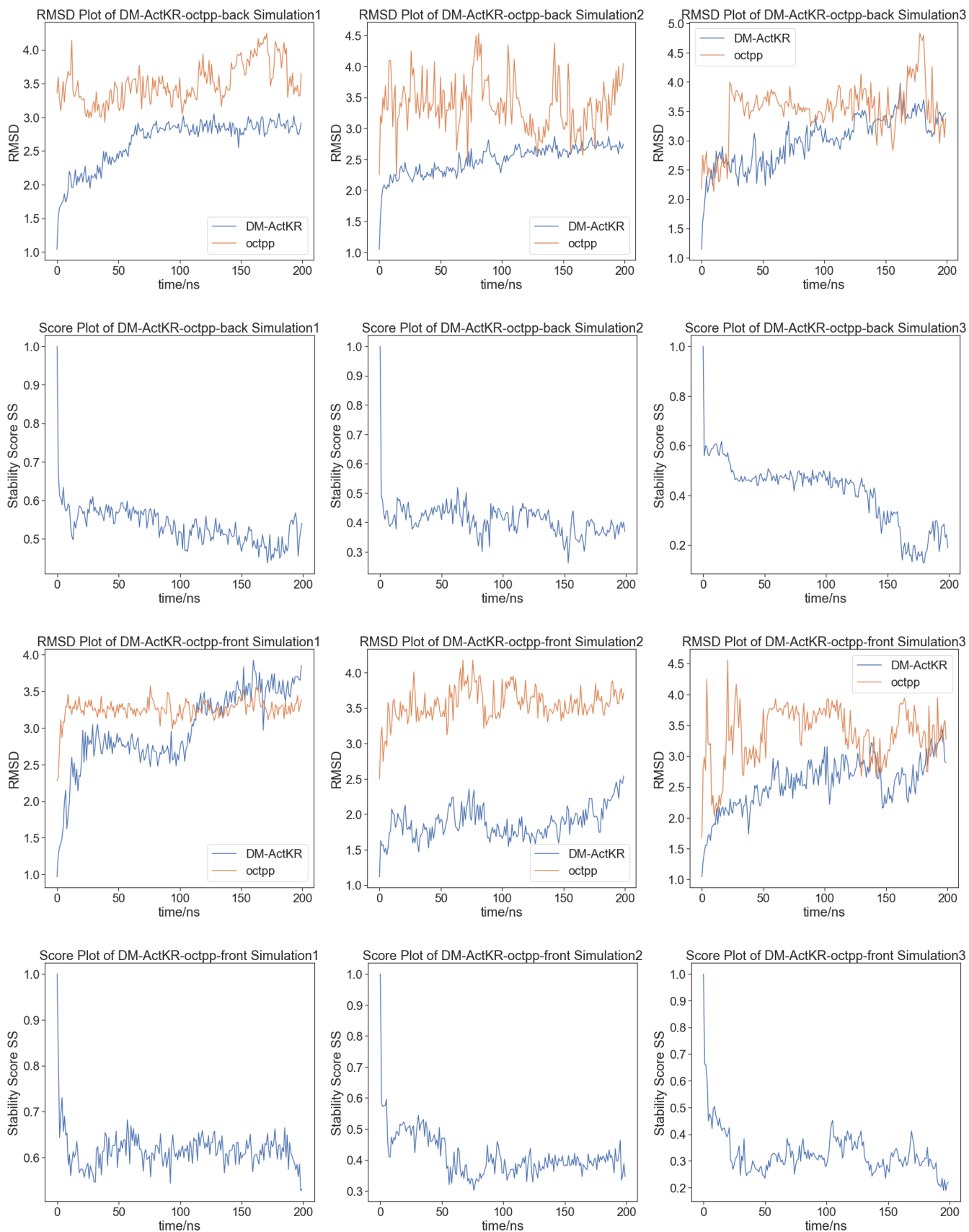


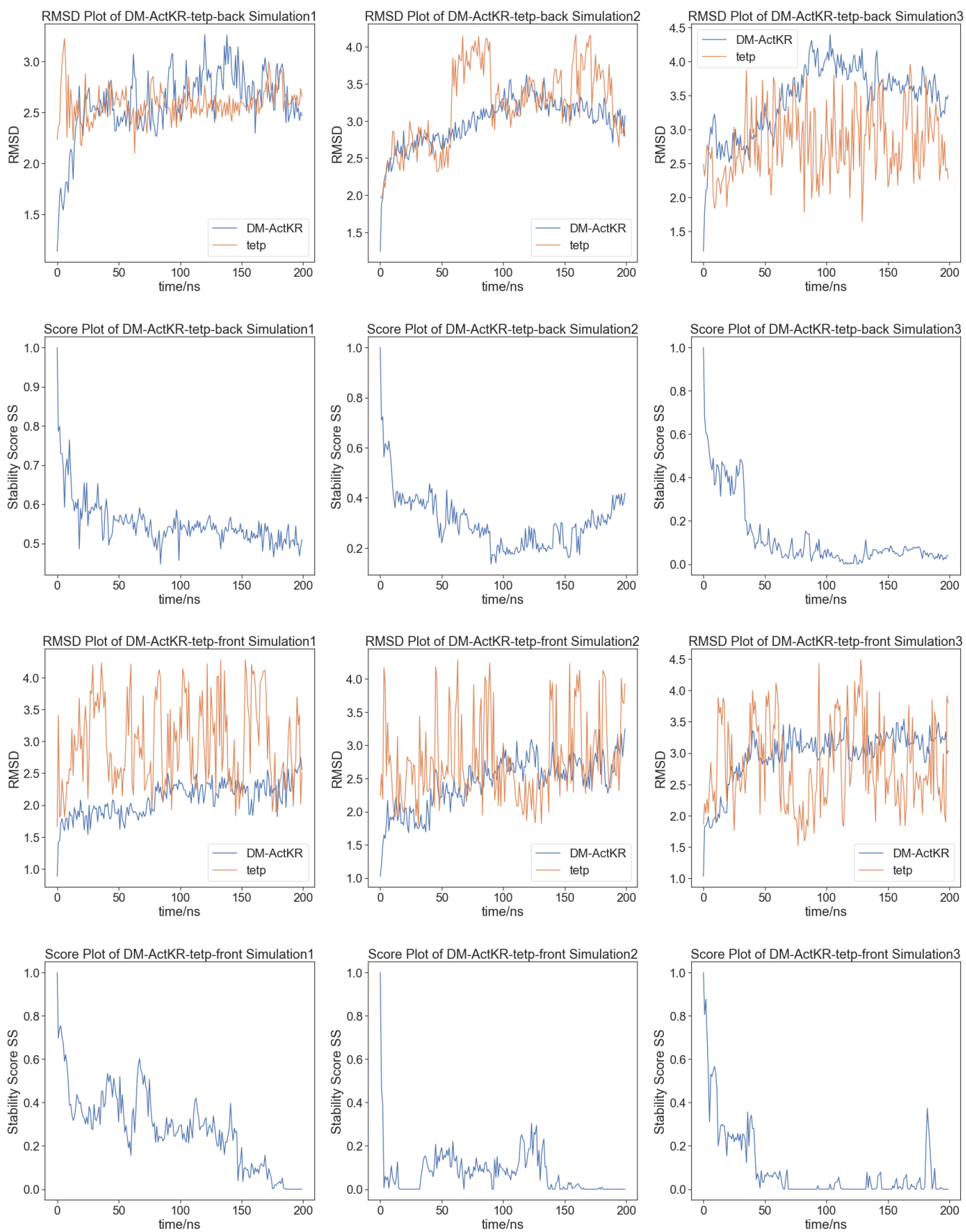


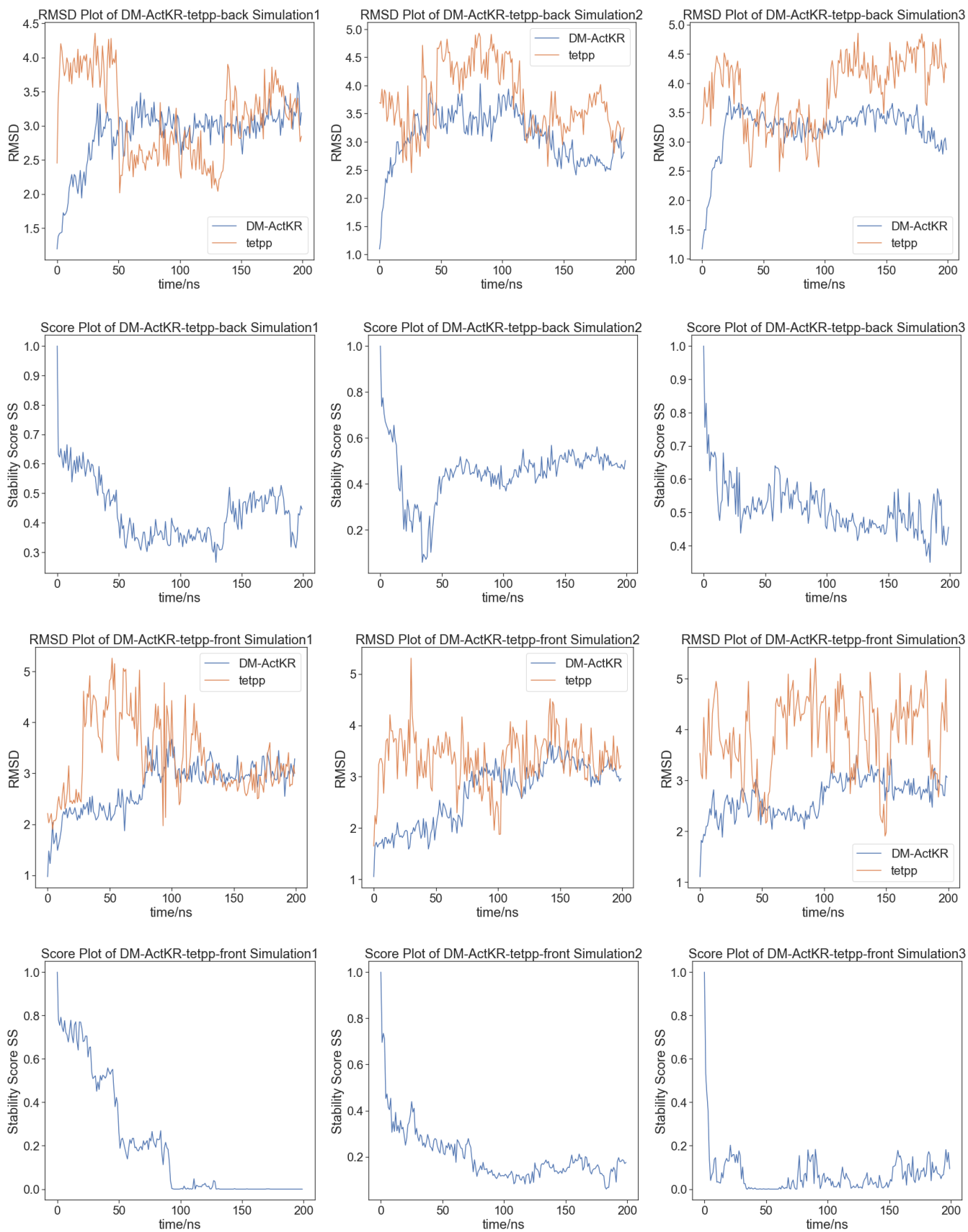


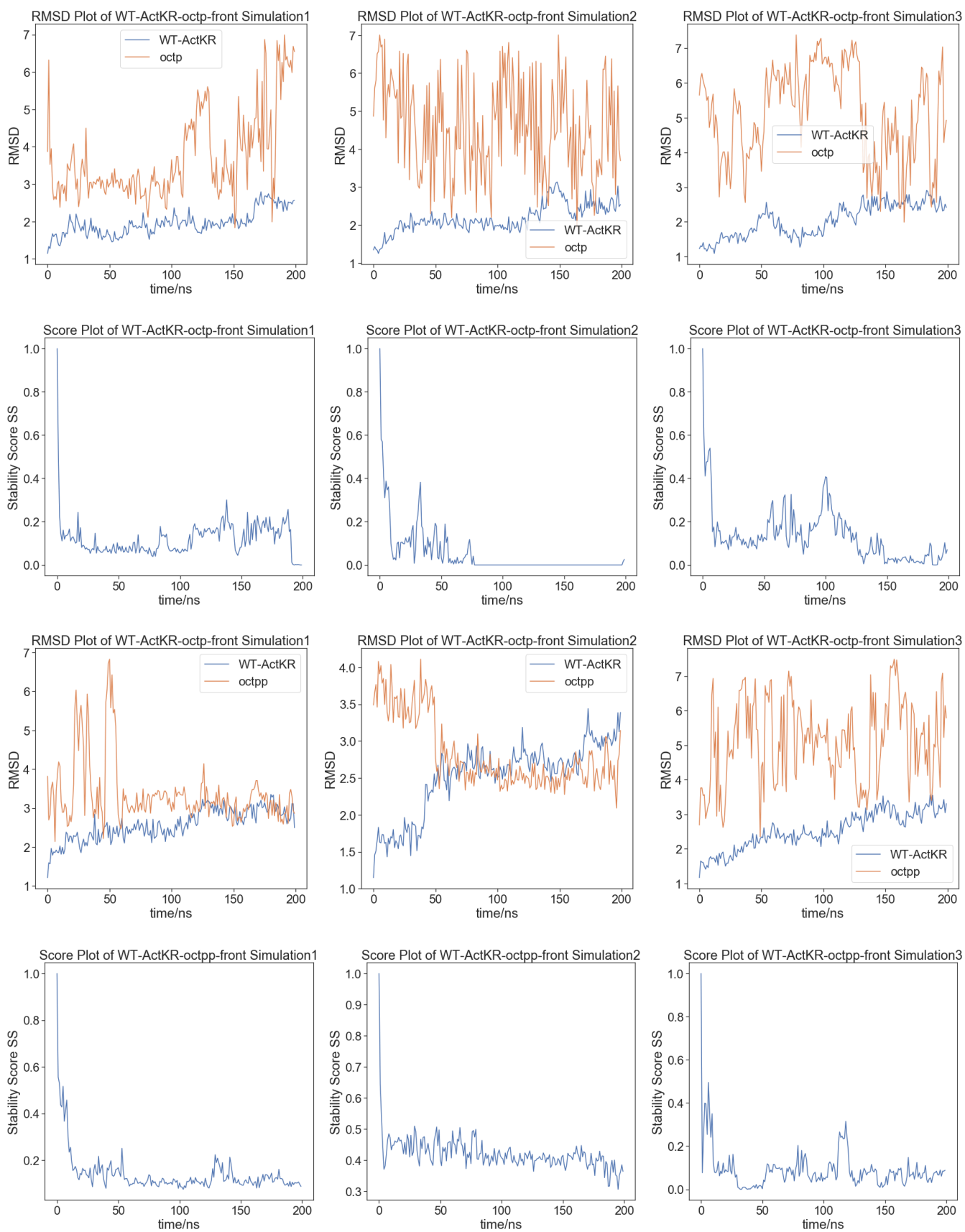


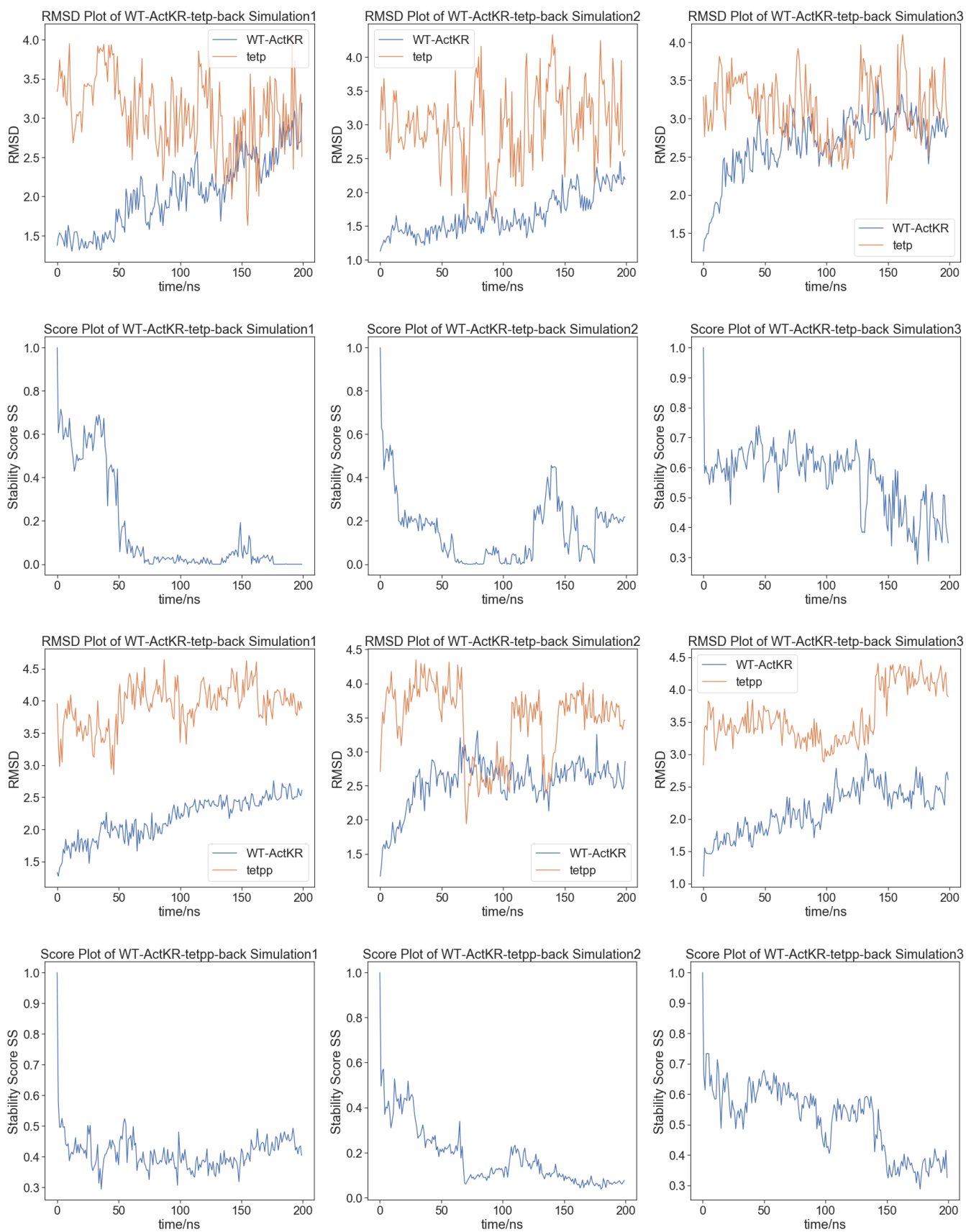


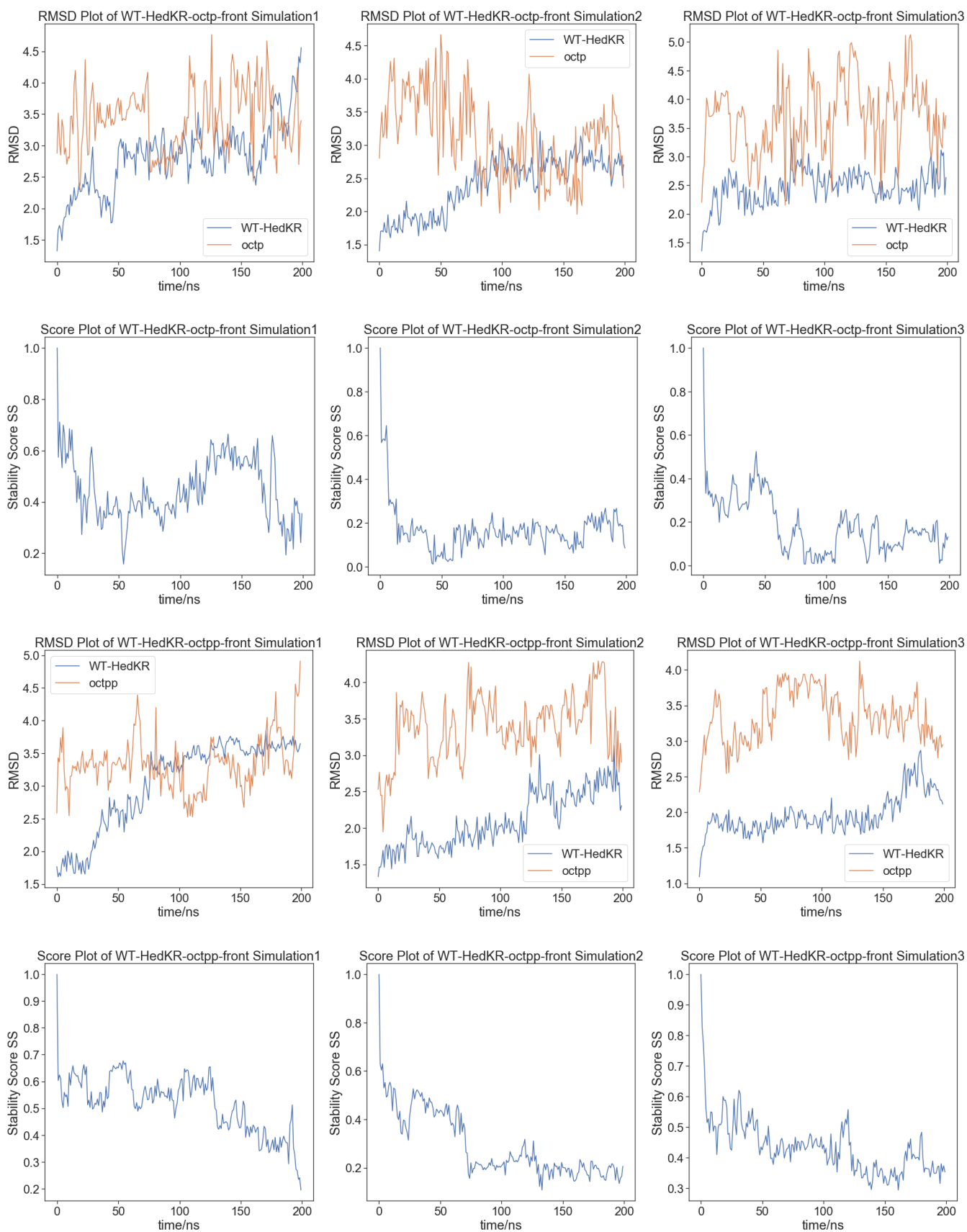












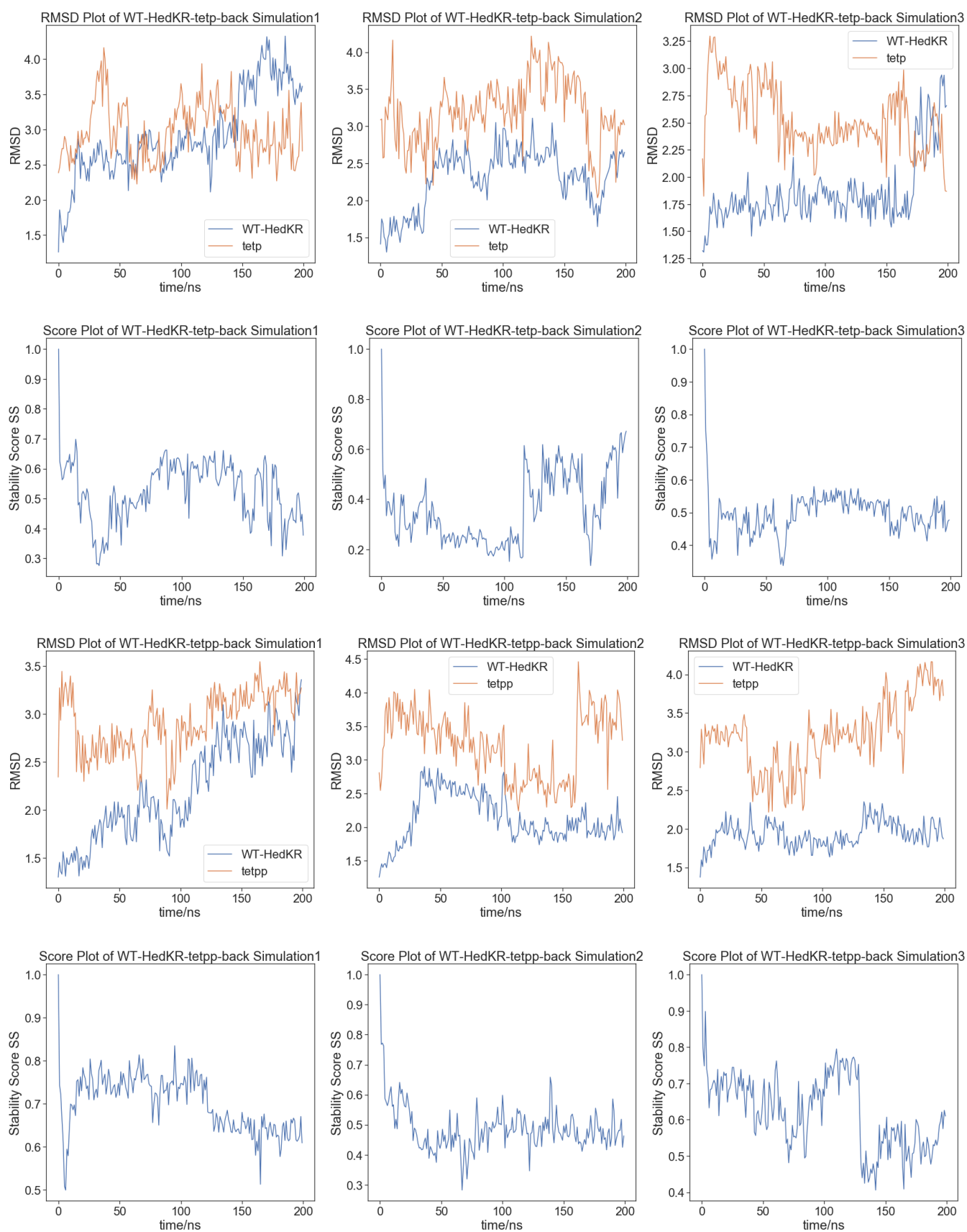


Figure S3. The RMSD and Stability Score SS_i plots of each simulation trajectory. The RMSD-simulation time plots have KR displayed in blue, ligands displayed in orange. The Stability Score SS_i -simulation time plots have Stability Score displayed in blue.

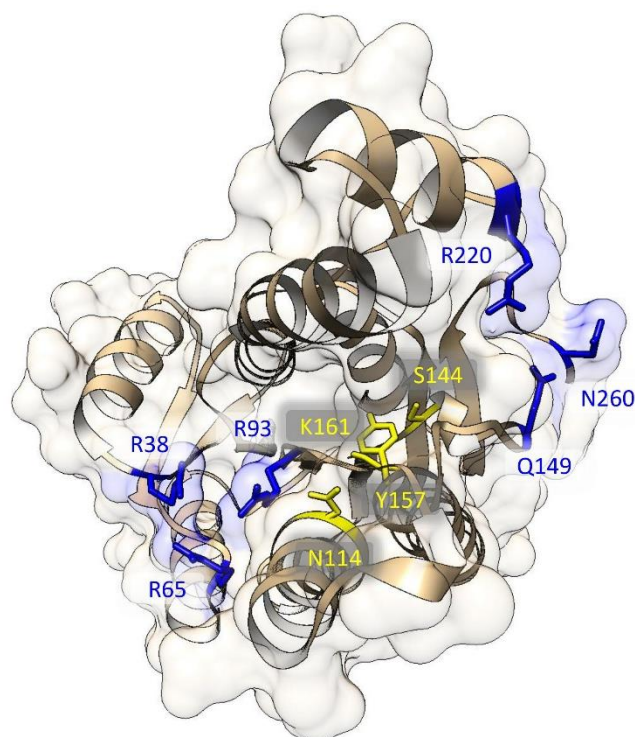


Figure S4. Front view of DM-AcrKR displaying the relative positions of front patch, back patch and catalytic residues. The front-patch (R38, R65, R93) and the back-patch (Q149, R220, N260) form two opposite entrances of a long channel, in which the catalytic residues (N114, S144, Y157, K161) of active site are located at the center. Patch residues are displayed in blue and active site residues are displayed in yellow.

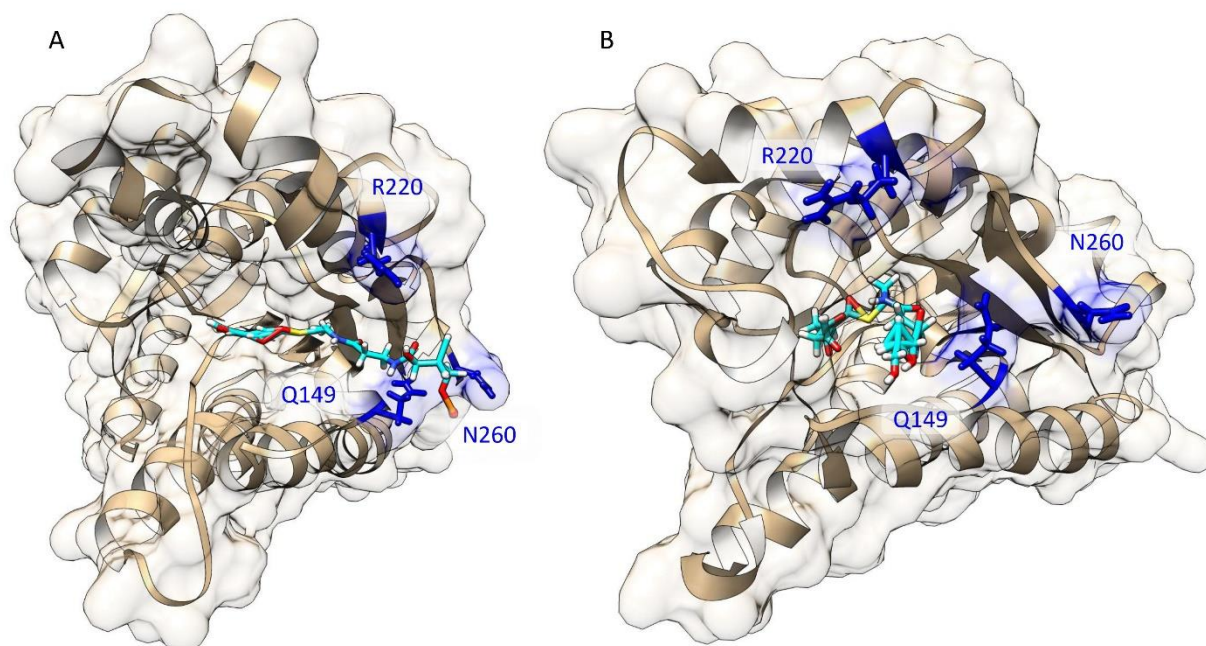


Figure S5. Hanging chain effect comparison between DM-AcrKR-tet-pp binding and DM-AcrKR-tet-p binding. Hanging chain effect is shown in DM-AcrKR-tet-pp binding (A) but not in DM-AcrKR-tet-p binding (A) Both figures show the average structure

of the last 100ns of the simulation trajectories. In (A), both ends of the ligand are constrained, and DM-ActKR is in open form. In (B), the pantetheine end of the ligand is not constrained, and DM-ActKR is in closed form.

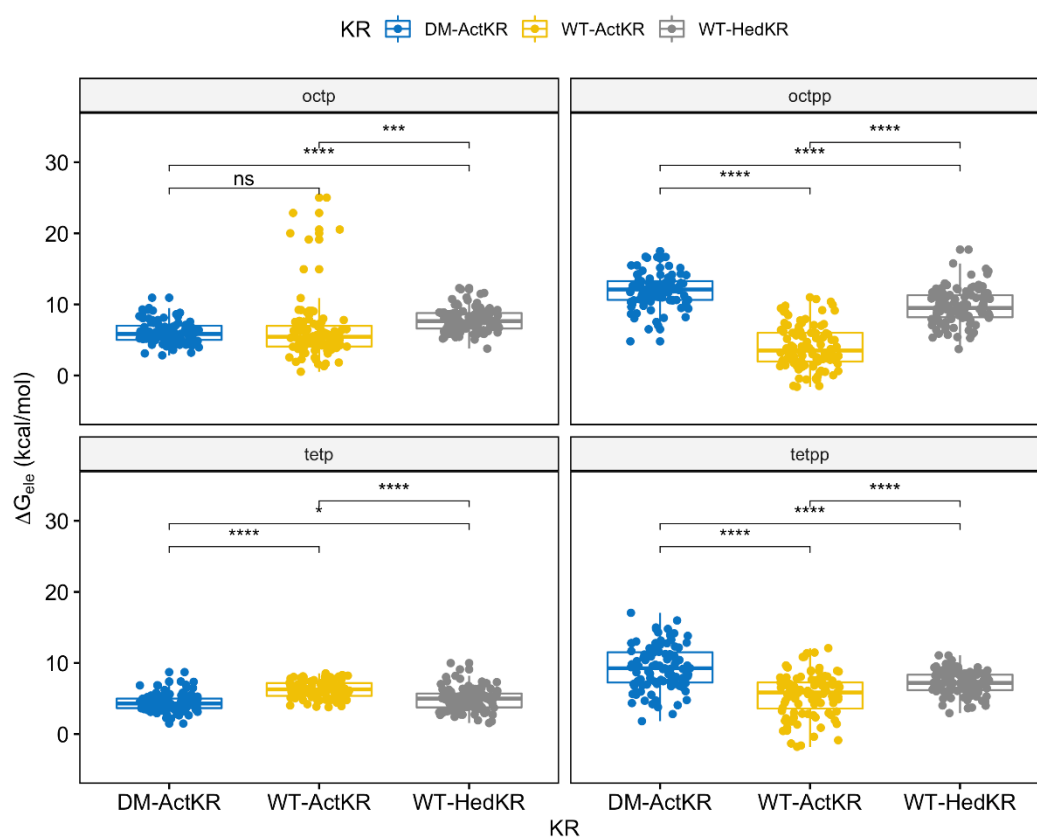
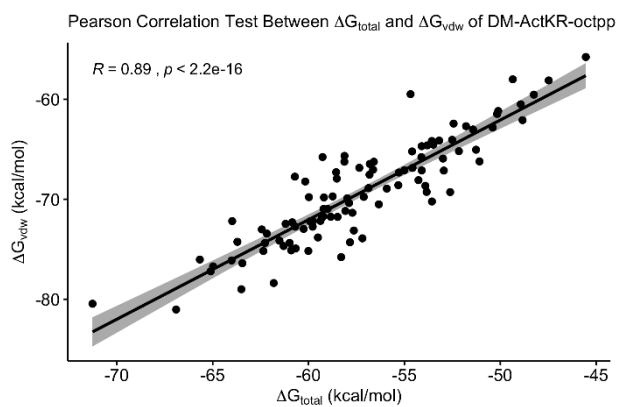
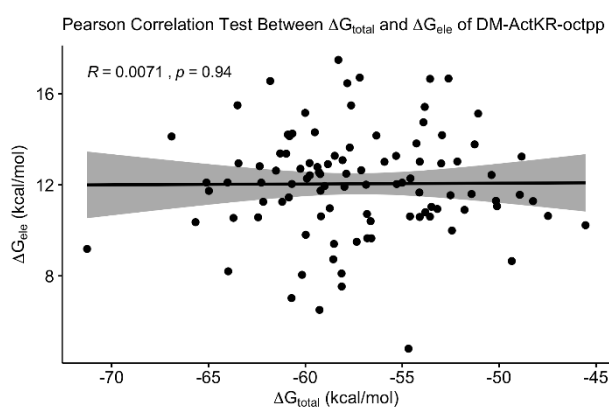
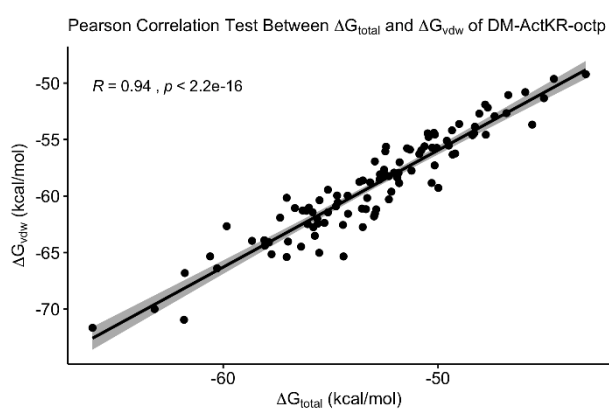
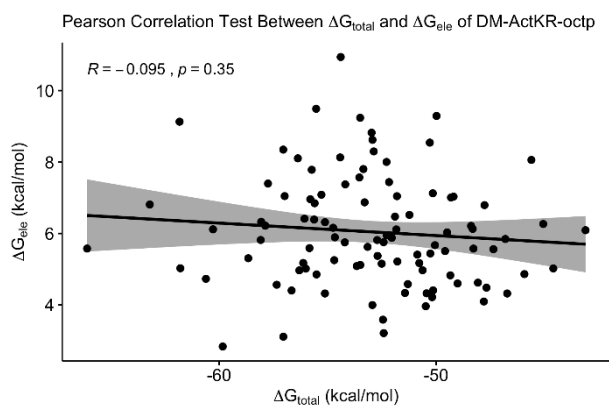
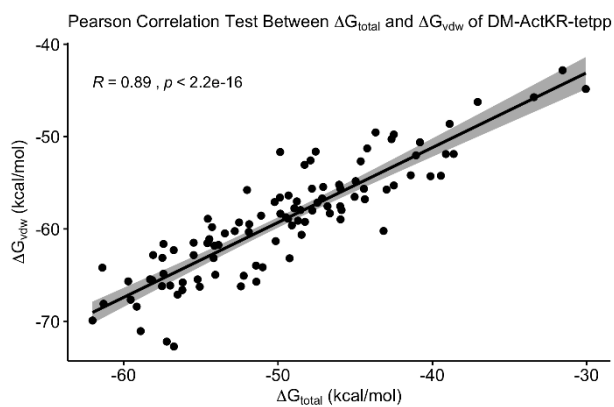
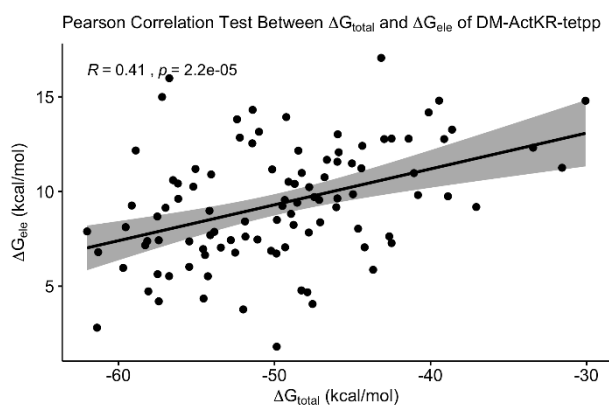
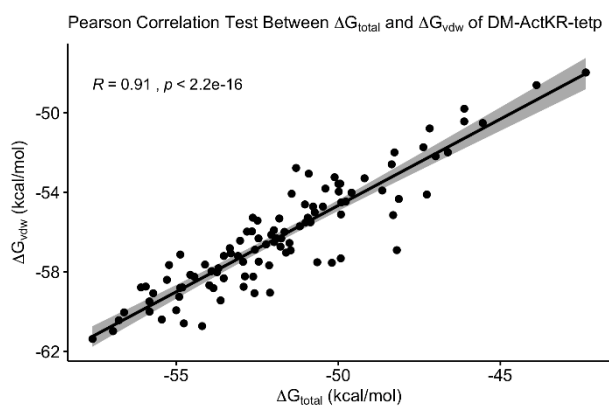
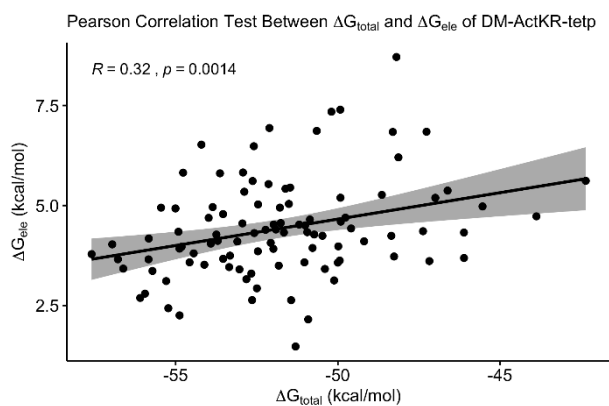
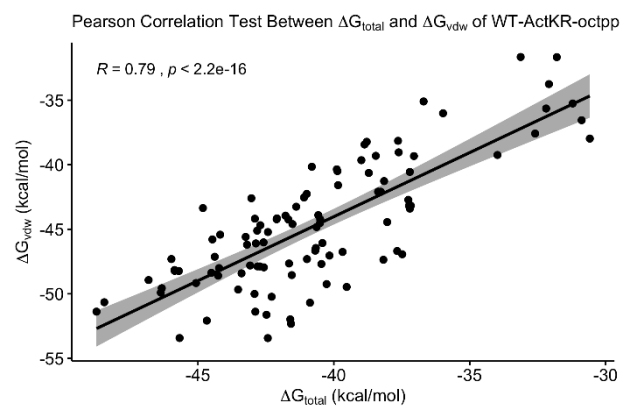
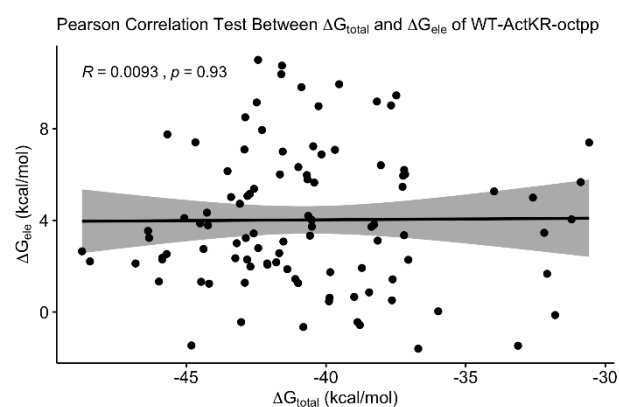
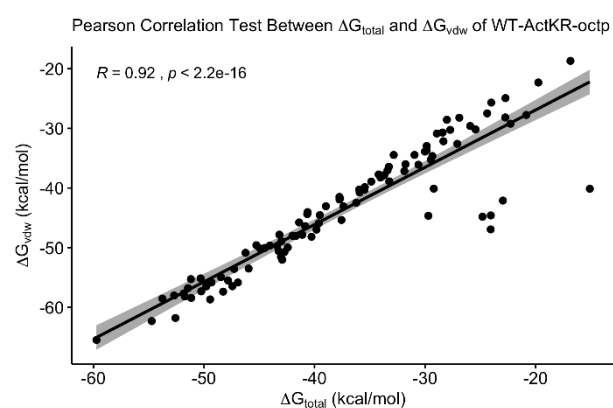
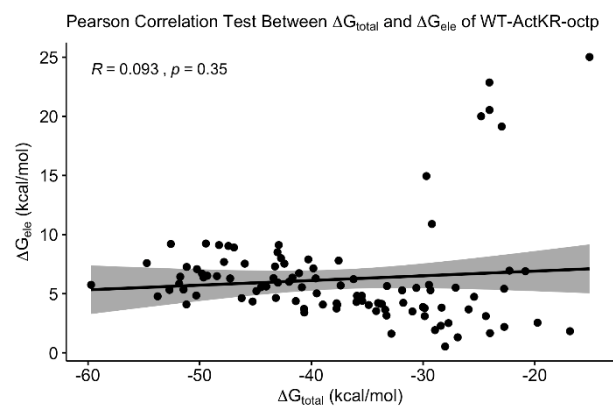
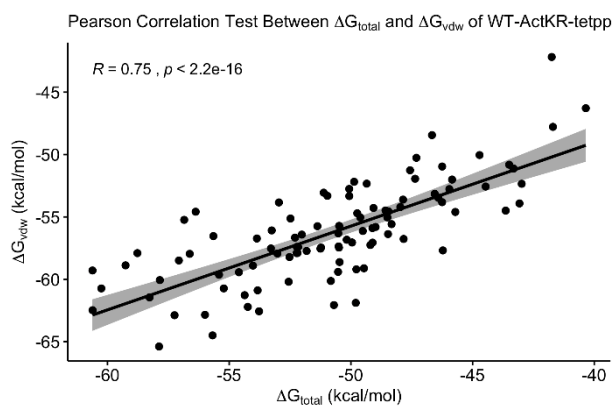
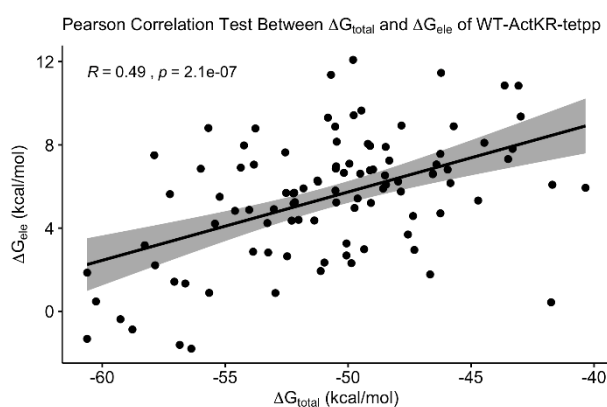
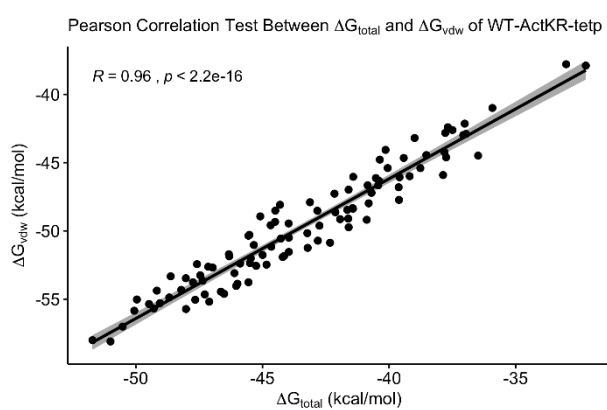
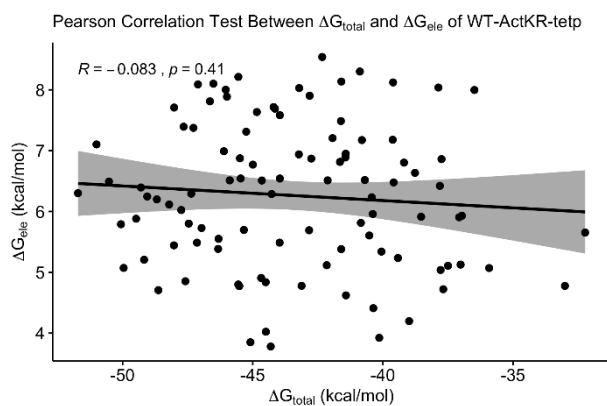


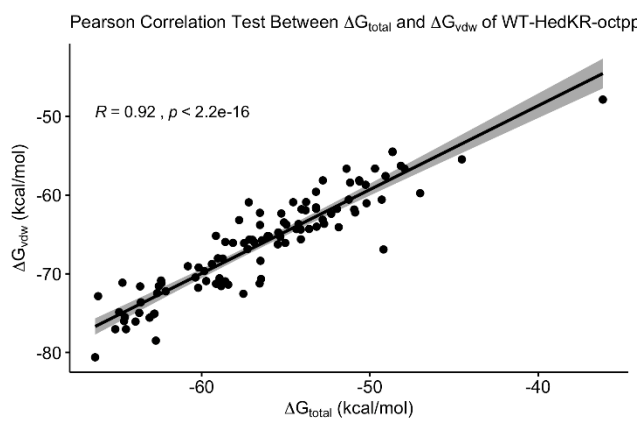
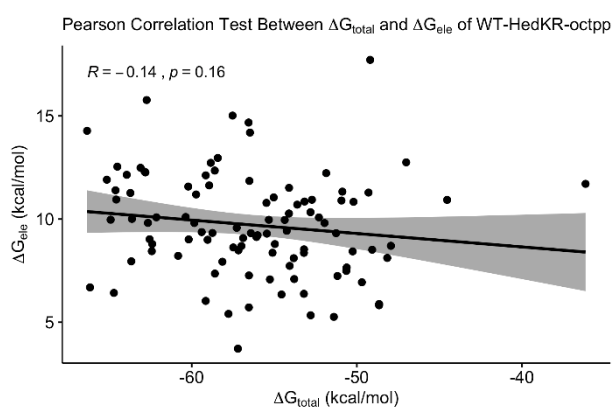
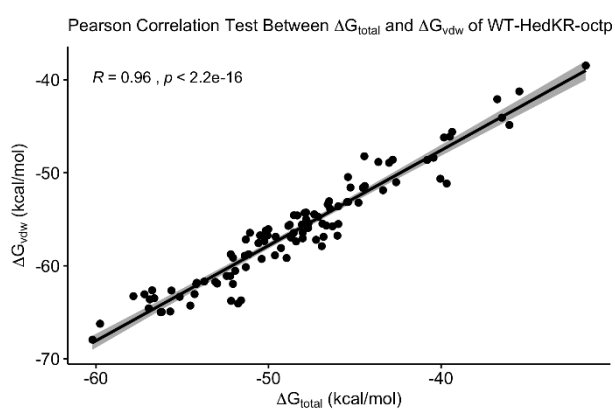
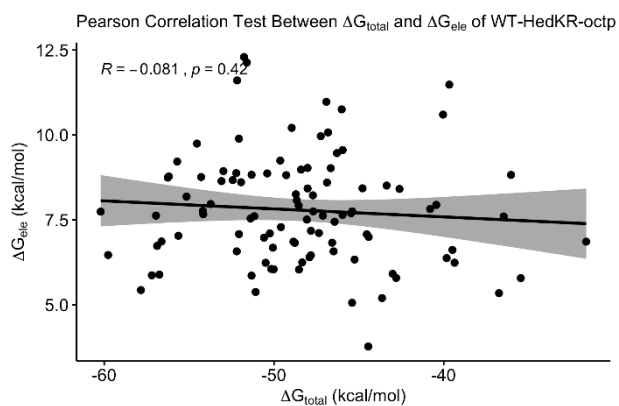
Figure S6. MMPBSA comparison of octaketides and tetraketides bound to DM-ActKR, WT-ActKR and WT-HedKR. Each box plot shows the electrostatic energy ΔG_{ele} results.











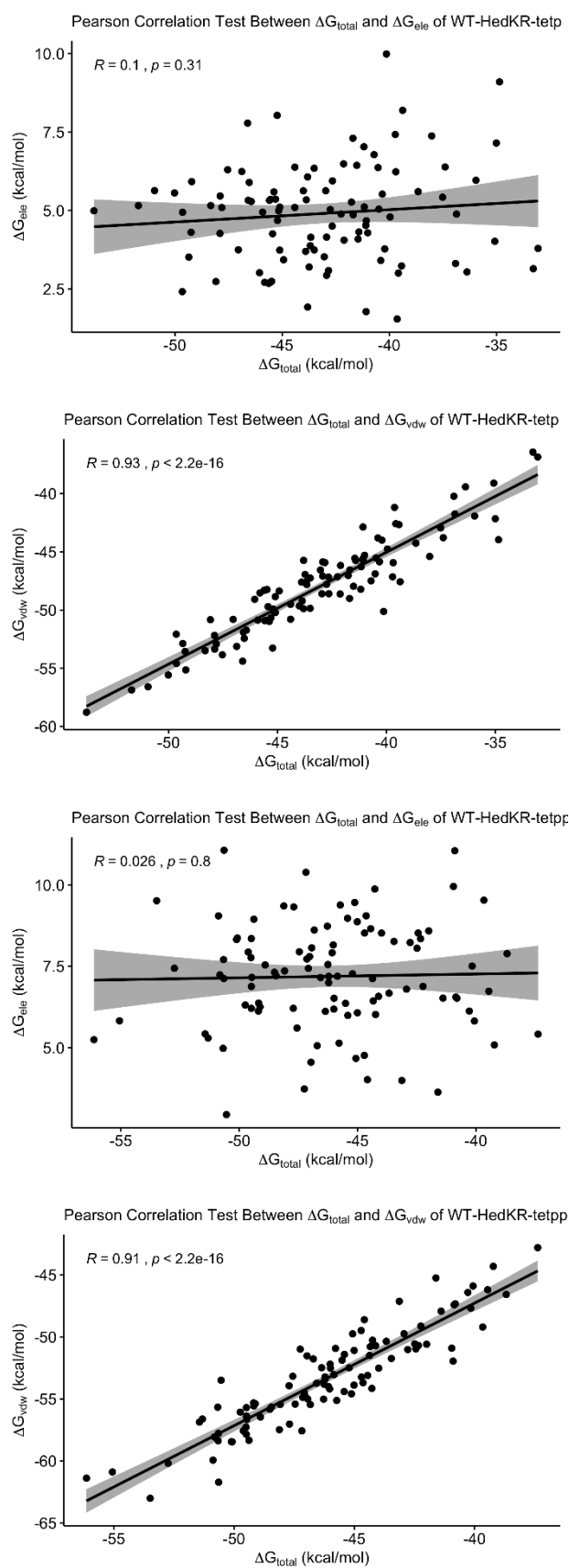


Figure S7. Framewise Pearson correlation test between ΔG_{total} with ΔG_{vdw} or ΔG_{ele} of each KR-ligand pair. ΔG_{total} is the total binding free energy; ΔG_{vdw} is non-electrostatic binding free energy; ΔG_{ele} is electrostatic binding free energy

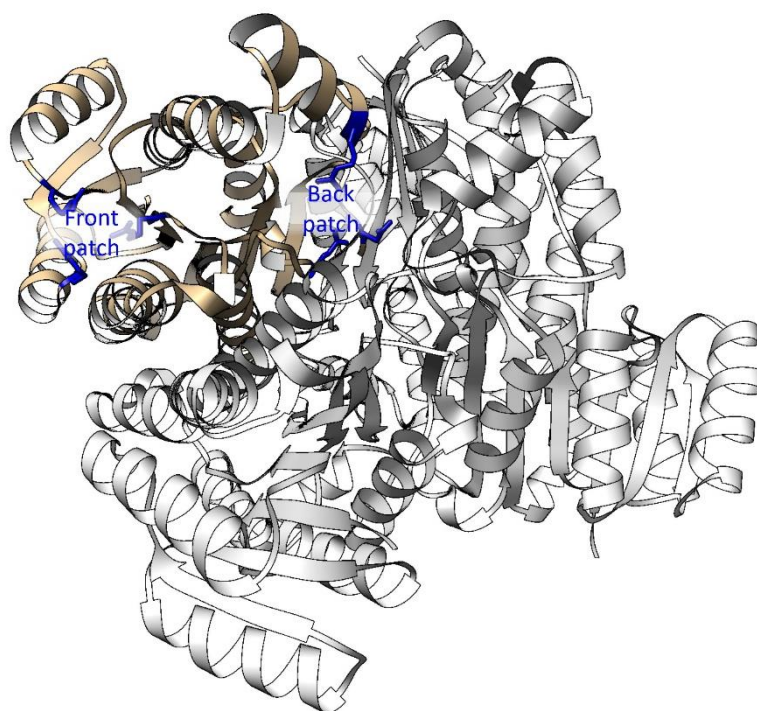


Figure S8. The position of the front patch and back patch in a native *ActKR* tetramer. Only the front patches (left) are exposed to the outer surface, while the back patches (right) are buried inside the interface between monomers, potentially occluding ACP binding. Front and back patches are displayed in blue.